HHS Public Access

Author manuscript

Stem Cells. Author manuscript; available in PMC 2017 February 01.

Published in final edited form as:

Stem Cells. 2016 July ; 34(7): 1896–1908. doi:10.1002/stem.2363.

Foxi3 deficiency compromises hair follicle stem cell specification and activation

Vera Shirokova[1], **Leah C. Biggs**[1,#], **Maria Jussila**[1,#], **Takahiro Ohyama**[2], **Andrew K. Groves**[3], and **Marja L. Mikkola**[1,*]

[1]Research Program in Developmental Biology, Institute of Biotechnology, University of Helsinki, P.O.B. 56, 00014 Helsinki, Finland [2]Department of Otolaryngology – Head & Neck Surgery and Zilkha Neurogenetic Institute, Keck School of Medicine, University of Southern California, 1501 San Pablo Street, Los Angeles CA 90033-4503 [3]Program in Developmental Biology, Department of Molecular and Human Genetics and Department of Neuroscience, Baylor College of Medicine, BCM295, 1 Baylor Plaza, Houston TX 77030

Abstract

The hair follicle is an ideal system to study stem cell specification and homeostasis due to its well characterized morphogenesis and stereotypic cycles of stem cell activation upon each hair cycle to produce a new hair shaft. The adult hair follicle stem cell niche consists of two distinct populations, the bulge and the more activation-prone secondary hair germ. Hair follicle stem cells are set aside during early stages of morphogenesis. This process is known to depend on the Sox9 transcription factor, but otherwise the establishment of the hair follicle stem cell niche is poorly understood. Here we show that that mutation of *Foxi3*, a Forkhead family transcription factor mutated in several hairless dog breeds, compromises stem cell specification. Further, loss of *Foxi3* impedes hair follicle downgrowth and progression of the hair cycle. Genome-wide profiling revealed a number of downstream effectors of Foxi3 including transcription factors with a recognized function in hair follicle stem cells such as Lhx2, Runx1, and Nfatc1, suggesting that the *Foxi3* mutant phenotype results from simultaneous downregulation of several stem cell signature genes. We show that Foxi3 displays a highly dynamic expression pattern during hair morphogenesis and cycling, and identify Foxi3 as a novel secondary hair germ marker. Absence of *Foxi3* results in poor hair regeneration upon hair plucking, and a sparse fur phenotype in unperturbed mice that exacerbates with age, caused by impaired secondary hair germ activation

[*]**Corresponding author:** Marja L. Mikkola, PhD, Address: Research Program in Developmental Biology, Institute of Biotechnology, University of Helsinki, P.O.B. 56, 00014 Helsinki, Finland, marja.mikkola@helsinki.fi, phone: +358-2-94159344, fax: + 358-2-94159366.

[#]equal contribution

Author contributions:

V.S.: study design, performance, data collection, analysis and interpretation, and manuscript writing

M.J. and L.C.B.: data collection, analysis and interpretation

T.O. and A.K.G.: provision of study material

M.L.M.: Conception and design of the study, data interpretation, and manuscript writing

DISCLOSURE OF POTENTIAL CONFLICTS OF INTEREST

The authors indicate no potential conflicts of interest.

leading to progressive depletion of stem cells. Thus, Foxi3 regulates multiple aspects of hair follicle development and homeostasis.

Keywords

Hair follicle stem cells; morphogenesis; ectodermal dysplasia; Shh

INTRODUCTION

Tissues and organs often use the same molecular mechanisms for morphogenesis and regeneration. As an organ capable of renewing throughout life, the hair follicle (HF) offers an excellent model to study the links between early developmental events and postnatal renewal. In mice, the induction of first (primary) HFs is marked by formation of epithelial placodes and mesenchymal condensates, precursors of dermal papilla (DP), at embryonic day 14.5 (E14.5) [1,2]. During morphogenesis, sebaceous gland emerges in the upper portion of the HF whereas the leading edges of the down-growing follicular epithelium encase the DP and form a population of transit amplifying (TA) cells, also called the matrix (Mx). The Mx gives rise to the multiple cell lineages of the hair shaft and its channel, the inner root sheath (IRS) [3,4]. The IRS is enveloped by the outer root sheath (ORS), which is contiguous with the basal layer of the interfollicular epidermis [2]. Hair morphogenesis is completed by around postnatal day 10 (P10), when the follicle reaches its maximal length. From this point onwards, two compartments can be distinguished in the HF: a lower cycling part and the upper permanent part. The lower part is renewed in every hair cycle, going first through apoptotic regression (catagen), followed by a rest stage (telogen), and a new growth phase (anagen) [5]. In each cycle, the lower portion is regenerated via a morphogenetic process reminiscent of the embryonic/early postnatal downgrowth of the follicle [2,6].

The cyclic regeneration of the HF is ensured by two populations of epithelial stem cells (SC), the bulge and secondary hair germ (HG), apparent as distinct anatomical entities only at telogen [7]. The bulge is an epithelial compartment in the lower part of the telogen HF. The HG lies just beneath the bulge in direct contact with the DP, which provides key signals for HF development and regeneration [8]. In homeostasis, the bulge and HG possess different functions and produce distinct progeny. At the onset of anagen, HG SCs are the first to be activated and to proliferate, and HG descendants give rise to the newly established Mx [3,9,10]. Bulge SCs start to proliferate 1–2 days later than the HG as the result of a positive signaling loop from the nascent TA cells [11]. The progeny of the lower bulge builds up the ORS [9,11]. During catagen, HG progeny, as well as most ORS cells die, but some slow-cycling ORS cells survive and contribute to the HG and the “new” bulge [3].

Molecular markers and transcription profiles of different HF stem and progenitor cell populations have been extensively characterized [6,12,13]. The HF and sebaceous gland SC niche displays extensive molecular heterogeneity. HF SC markers include keratin 15 (K15), Lgr5, and transcription factors Sox9 and Lhx2 that are expressed both in the bulge and HG [6,13]. However, also markers unique to bulge or HG cells have been identified: CD34 and Nfatc1 are restricted to bulge [14,15], whereas P-cadherin and Runx1 are enriched in HG

[16,17]. Thus, current evidence indicates that the bulge and HG represent biochemically and functionally separate populations. The HF SC niche displays a great level of plasticity though, since following physical ablation of one of the populations both bulge and HG are able to functionally substitute each other and to regenerate the follicle [9].

While the composition of the adult HF SC niche is well-described, its establishment during development is poorly understood. *Shh*-expressing placode cells give rise to all cell types of the HF, including the bulge [18]. Pulse-chase experiments have revealed that slow-cycling cells appear in the upper portion of primary HFs (pre-bulge) already during late embryogenesis and give rise to the adult bulge [19]. One of the earliest markers for these cells is Sox9, which is essential for the formation and maintenance of SCs [19–21]. In late embryogenesis, Sox9-expressing cells in the future bulge compartment also express the telogen SC markers Lhx2, Nfatc1, and Tcf3 [19], but the exact hierarchy between these genes in early HF SC specification is not fully understood. In cycling HFs these transcription factors have important functions in controlling the switch between SC quiescence and activation [15,21–25].

Hair morphogenesis and renewal are driven by the same key signaling pathways [2,6,8]. Wnt/BMP balance is crucial for the developing HF as well as for postnatal hair regeneration. Downregulation of Wnt signaling by overexpression of the inhibitor Dkk1, or deletion of epithelial β-catenin, results in complete block of initiation of hair development [26]. Suppression of Bmp signaling is essential for hair placode induction and expression of Lef1 [27–29]. Similarly, downregulation of BMP and upregulation of Wnt signaling in the adult HF SCs are also two key events for telogen to anagen transition [25,30–34].

There is also an absolute requirement for Sonic hedgehog (Shh) in follicle downgrowth since morphogenesis is arrested soon after placode formation in *Shh* null mice [35,36]. During hair cycling, Shh, produced by TA cells (the HG progeny) ensues anagen progression after the initial HG activation by intensifying expression of soluble DP factors. Further, it instructs bulge SCs to proliferate [11]. Also epithelial Fgf signaling has been implicated in HF downgrowth, as mice lacking Fgfr2-IIIb have fewer and less well developed HFs at birth [37]. In postnatal hair, FgfR2-IIIb ligands FGF7/10 emitted from the DP provide proliferation signals to the HG cells [10,11].

Another important pathway involved in hair development is the ectodysplasin (Eda)/NF-κB pathway [38]. We have previously identified transcription factor *Foxi3* as an Eda target gene in hair placodes [39]. In dogs, *Foxi3* haploinsufficiency leads to ectodermal dysplasia characterized by near total hairlessness [40,41]. In this study, we genetically dissect the role of Foxi3 in hair morphogenesis and regeneration using mouse models and show that Foxi3 regulates multiple aspects of HF biology.

MATERIALS AND METHODS

Animals

Transgenic mouse lines used in this study have been described earlier: K17-GFP mice [42], NF-κB reporter [43], BAT-gal [44] were maintained on a C57Bl/6 background.

Foxi3$^{+/-}$ [45] mice were maintained on ICR and C57Bl/6 backgrounds, and *Foxi3*$^{floxed/floxed}$ mice (the Jackson laboratory, stock no. 024843) on the ICR background. Transgenic K14-Cre43 [46] and knock-in K14-Cre [47] mice were used to generate conditional *Foxi3* mutants (carrying one null and one floxed allele) in a mixed NMRI/ICR background. Inducible *Foxi3* cKO mutants (also carrying one null and one floxed allele) in a mixed background were generated with the aid of K14-CreERT (Jackson laboratory, stock no. 005107) or Lgr5$^{CreIRES-GFP-ERT2}$ (Jackson laboratory, stock no. 008875). Cre recombinase was activated at postnatal day 56–62 by 5 daily injections of tamoxifen (0.75–1.5 mg/10g) diluted in corn oil (Sigma Aldrich). Foxi3$^{+/+}$ and Foxi3$^{+/floxed}$ were mostly used as a controls. For the microarray and qRT-PCR all controls were Foxi3$^{+/+}$. For embryonic samples, the day of the vaginal plug was considered as E0.5, and the embryos were further staged according to limb morphology and other external criteria. For skin transplantation, E18.5 dorsal skin was dissected and grafted onto Nude mice (HsdCpb:NMRI-Foxn1^{nu}; Harlan Laboratories) as previously described [48]. All mouse work was approved by the Finnish National Board of Animal Experimentation.

Histology, in situ hybridization, immunohistochemistry, immunofluorescence, X-gal staining, and microscopy

Paraformaldehyde (4%) fixed tissues were embedded into paraffin, and sections of 5–7 μm were used for histology, radioactive in situ hybridization (RISH), and immunohistochemisty. Whole mount ISH (WMISH) was performed on E14.5 embryos using a digoxigen-labeled RNA probe to *Foxi1, Foxi2*, or *Foxi3* [49]. RISH was completed on sections using ^{35}S-UTP (Amersham) -labelled RNA probe to *Foxi3* and *Shh* [50]. RISH and WHISH were performed as previously described [39].

For cell proliferation assay, BrdU (Amersham) was injected intraperitoneally at 10 μl/g, mice were sacrificed 2 hours later. For BrdU detection, tissue sections were treated with 0,6% H_2O_2 for 30 min at room temperature, in 1mM HCl for 15 min at 37°C, incubated with BrdU antibodies, stained with MOM immunodetection kit (Vector Laboratories) and DAB peroxidase substrate kit (Vector Laboratories). For all antibodies, antigen retrieval was performed in heated Na-citrate buffer (pH 6.0) for 10 min. All samples were imaged with Zeiss Axio Imager M2 microscope equipped with Axio Cam HR camera (Zeiss, Jena, Germany) and the images processed in Photoshop. Antibodies are listed in Supplementary Information.

X-gal staining on E14.5-E18.5 whole embryos or dissected skin was according to standard protocols [48]. The samples were imaged with Olympus SZX9 stereomicroscope equipped with a V-CMAD3 camera.

Scanning electron microscopy (SEM) was performed on plucked hairs coated with platinum (Agar Sputter Coater, Agar Scientific, Stansted, UK) and imaged with Zeiss DSM 962 scanning electron microscope (Zeiss, Oberkochen, Germany) at the Electron Microscopy Unit of the University of Helsinki.

Tissue culture

Skin explants from E14.5 *Foxi3*$^{-/-}$;K17-GFP and K17-GFP control littermates were cultured as previously described [48] w/wo the following recombinant proteins: Wnt3A (R&D Systems, 10 ng/ml), R-spondin2 (R&D Systems, 100 ng/ml), Fgf8 (R&D Systems, 500ng/ml), Fgf10 (R&D Systems, 500 ng/ml), or BSA (Sigma Aldrich, 5μg/ml) as a control.

Microarray analysis and qRT-PCR

For microarray analysis of differentially expressed genes upon loss of *Foxi3*, the epithelia from four E15.5 *Foxi3*$^{-/-}$ and four *Foxi3*$^{+/+}$ littermates from four different litters on C57Bl/6 background were isolated after incubation in 0.2 U/ml Dispase II (Sigma Aldrich) for 4 hours at +4°C. Epithelia were stored in RNA-later (Qiagen), followed by RNA isolation with RNeasy micro-kit (Qiagen). RNA quality was checked with 2100 Bioanalyzer, and samples with RIN 9.6–10 were used for microarray. RNA hybridization on Affymetrix Mouse Exon 1.0 ST arrays and data analysis were conducted in the Biomedicum Functional Genomics Unit (University of Helsinki). The data were processed using R/Bioconductor and normalized with RMA algorithm and CustomCDF-database probe annotations. Differentially expressed genes were identified using Cyber-T algorithm. P-values were corrected using Q-value method. Microarray data are available in GEO (GSE68985).

For validation of the microarray results, qRT-PCR of the selected genes was performed using six *Foxi3*$^{-/-}$ and six Foxi3$^{+/+}$ samples. RNA was extracted as described and reverse transcribed using 500 ng of random hexamers (Promega, Fitchburg, WI, USA) and Superscript II (Invitrogen by LifeTechnologies, Thermo Fisher Scientific) following manufacturers' instructions. qRT-PCR was performed using Lightcycler DNA Master SYBR Green I (Roche Applied Science, Basel, Switzerland) with the Lightcycler 480 (Roche Applied Science, Basel, Switzerland). Gene expression was quantified from calibration curve from the standards of diluted PCR products of the gene of interest, analysed with the software provided by the manufacturer and normalized to *Ranbp1*. Primers are listed in Supplementary Information.

RESULTS

Foxi3 displays dynamic expression pattern during hair morphogenesis and cycling

We previously showed that *Foxi3* mRNA expression is confined to the epithelium of embryonic HFs at the placode stage [39]. Staining with a Foxi3 antibody, whose specificity was validated using *Foxi3*-null samples (see below; Fig. S1A, S1B), confirmed these findings, and there was a good correlation between mRNA and protein expression in developing and cycling HFs (Fig. 1). In more advanced follicles, expression of Foxi3 waned and was observed only in a subset of cells in the center of the follicle above the Mx (Fig. 1B, 1C). In fully formed follicles, Foxi3 was no longer detectable (Fig. 1D). However, expression reappeared at catagen, in the cells of the epithelial strand, and got restricted to HG at telogen (Fig. 1E, 1F). At the onset of anagen, Foxi3 expression expanded into TA cells (Fig. 1G), but, similar to morphogenesis, was no longer discernible in more advanced anagen follicles (Fig. S1C).

To further characterize Foxi3-expressing cells, we performed immunostaining of Foxi3 in combination with Lhx2, Nfatc1, and Sox9 during morphogenesis and in telogen HFs (Fig. 2). Foxi3 was coexpressed with Lhx2 at placode and germ stage, but at advanced stages Foxi3+ cells in the center of the follicle were negative for Lhx2 (Fig. 2A). Nfatc1 was not observed at placode stage, but appeared in the upper outer root sheath at peg stage in cells that also expressed Foxi3 (Fig. 2B). Later at the bulbous peg stage, Foxi3 and Nfatc1 no longer colocalized (Fig. 2B). Sox9 and Foxi3 were coexpressed in some cells of the placode, at the upper portion of the hair peg and in the center of the HF (Fig. 2C). These cells were distinct from the IRS precursors marked by Gata3 (Fig. S1D). At telogen, Lhx2 and Sox9, but not Nfatc1, were coexpressed with Foxi3 in the HG (Fig. 2A–2C).

Normal patterning but delayed downgrowth of hair follicles in Foxi3-null embryos

To assess the function of Foxi3 in HF development, we analyzed *Foxi3* null mice (hereafter *Foxi3* KO) [45]. Surprisingly, in the outbred ICR background, homozygous embryos (up to P0) displayed no apparent HF phenotype (data not shown). We examined the expression of the related *Foxi1* and *Foxi2* genes by in situ hybridization, but did not detect any signal in wild-type or *Foxi3* KO embryos (Fig. S2). In C57Bl/6 background, however, loss of *Foxi3* had a noticeable effect on HF development and these mice were used for further analyses (see below). Similar to ICR, heterozygotes were indistinguishable from wild-type mice. These data suggest the presence of a compensatory mechanism for Foxi3 deficiency in ICR, but this seems not to involve redundancy with other *Foxi* genes.

In the C57Bl/6 background, primary hair placodes were induced normally in *Foxi3* KO embryos (Fig. 3A). However, a day later at hair germ stage, impaired invagination of the mutant hair buds was evident (Fig. 3B). The downgrowth phenotype persisted throughout embryogenesis, and prior to birth, the average length of the *Foxi3* KO HFs was only 65% of the control HFs, and a ~20% reduction in HF number was also observed (Fig. 3C–3E). To elucidate the mechanism behind the impaired downgrowth, we analyzed cell proliferation and cell death in Foxi3 KO hair follicles. There was a statistically significant decrease in the number of BrdU incorporating cells at E15.5, but not at late embryogenesis (Figs. 3F-3H). No difference in the active caspase-3 staining was observed at any stages analyzed (Fig. S3). These data imply that the reduced size of Foxi3 KO HFs is due an early proliferation defect.

Foxi3 KO mice die perinatally due to gross craniofacial malformations [45]. To follow postnatal HF morphogenesis, we grafted control and *Foxi3* KO embryonic skins to the dorsum of immunocompromised Nude mice (Supplementary Table S1). Retarded downgrowth of HFs was noticeable in Foxi3 KO explants at 10 days post-grafting, but no other dramatic morphological defects were observed (Fig. 3I). After three weeks, control transplants gave rise to bundles of hairs, while only few hairs grew in *Foxi3* KO grafts (Fig. 3J). Taken together, these data indicate that absence of *Foxi3* compromises HF downgrowth ultimately leading to failure in hair shaft formation.

Wnt, NF-κB, and Shh pathways are not affected by loss of *Foxi3*, and *Foxi3* deficiency cannot be rescued by exogenous Fgfs or Wnts

Given the importance of the Wnt/β-cat, Eda/NF-κB, and Shh pathways in hair development, we next looked for differences in their activity in *Foxi3* KO embryos. No changes in NF-κB reporter expression was detected in *Foxi3* KO HFs (Fig. S4A). Likewise, comparison of BAT-gal transgene [44] activity suggested that canonical Wnt signaling was unaffected (Fig. S4B, S4C). This conclusion was strengthened by the analysis of Lef1, a readout of Wnt signaling, which was similar in control and *Foxi3* KO HFs (Fig. 3K). No changes in *Shh* expression were detected either (Fig. S4D, S4E).

To further explore the molecular mechanisms that might explain *Foxi3* KO phenotype, we took advantage of the ex vivo skin culture system and tested the ability of Wnt and Fgf pathways agonists to rescue the downgrowth defect. To this end, we crossed the keratin17-GFP (K17-GFP) transgene [42] into Foxi3$^{+/-}$ background which allowed an easy visualization of the downgrowth phenotype (Fig. S5A). In E14.5 control back skins cultured for three days HFs grew significantly, whereas in *Foxi3* KO explants follicles displayed little growth and eventually many of them degenerated (Fig. S5B). No rescue was obtained with a Wnt3A/R-spondin2 treatment, or with Fgf10 (Fig. S5C, S5D). We recently reported that Fgf8 lies downstream of Foxi3 in pharyngeal ectoderm [45]. Therefore, we also tested Fgf8 which encages mesenchymally expressed IIIc isoforms of Fgf receptors [51]. Fgf8 had no impact on the growth of mutant HFs (Fig. S5E). Together these findings suggest that gross alterations in Wnt/β-cat, Eda/NF-κB, Fgf, or Shh signaling are unlikely to explain the *Foxi3* KO morphogenesis defect.

Gene expression profiling reveals a number of hair follicle SC signature genes downstream of Foxi3

To elucidate the molecular mechanisms involved in *Foxi3* KO hair phenotype, we performed genome-wide profiling of genes differentially expressed in back skin epithelia dissected from *Foxi3* KO embryos and their wild-type littermates at E15.5, when the KO phenotype was first apparent. Around 500 genes were differentially expressed (GSE68985; Supplementary Table S2). A majority of the genes (approx. 400) were downregulated, suggesting that in hair development, Foxi3 mostly operates as a transcriptional activator. Among the genes with a known or suspected function in HF biology, very few genes were associated with early morphogenesis. Instead, many have been implicated in HF SC function such as *Lhx2, Runx1, Klf4*, and *Nfatc1* [15,17,22,52].

To validate the microarray data, we performed qRT-PCR on selected genes with a known link to HF biology (Fig. 4A). Two genes expressed in hair placodes *Dkk4* and *PTHrP* [53], were up- and downregulated, respectively, in *Foxi3* KO epithelium. We showed statistically significant downregulation of *Lhx2, Nfatc1*, and *Runx1*, as well as *Hairless* (*Hr*) and *Lipase, member H* (*LipH*) genes, which are known regulators of HF cycling [54,55] (Fig. 4A). All 10 genes (including *Foxi3*) examined showed the same trend as in the microarray, the difference between wild-type and *Foxi3* KO specimen being statistically significant for 8 genes.

Early specification of the SC compartment is affected by Foxi3 deletion

The downregulation of several SC markers in *Foxi3* KO embryos prompted us to analyze these and other SC markers more in detail. Downregulation of Lhx2 and Nfatc1 was also evident at the protein level at E15.5 (Fig. 4B, 4C) suggesting that the initial specification of SC precursors may be affected in the absence of Foxi3. Next, we focused our analysis on later stages of embryogenesis, when the future bulge is forming [19]. *Foxi3* KO HFs showed normal staining for Lhx2 and Sox9, although the typical epithelial bulging marking the presumptive SC niche was not observed in mutants (Fig. 4D, 4E). In contrast, Nfatc1 was still strongly downregulated and appeared in *Foxi3* KO only at late morphogenesis (Fig. 4F, 4G). The adult SC marker keratin 15 (K15), was also significantly decreased in *Foxi3* KO HFs (Fig. 4E, 4F, 4H). Collectively, these data indicate at least a partial SC lineage failure in the absence of Foxi3.

Conditional Foxi3 deletion impairs postnatal hair growth and hair cycling

To study the long-term consequences of *Foxi3* deficiency we generated K14-Cre; *Foxi3*$^{null/floxed}$ conditional Foxi3 knock-out mice (hereafter *Foxi3* cKO). We used two different K14-Cre strains, a knock-in [47] and a transgenic [46]. Both mutants displayed the same gross phenotype and histologically similar hair cycling defect (Figs. 5, S6). All further analyses were completed using the transgenic Cre driver.

Foxi3 cKO mice were born in a Mendelian ratio, were viable, but smaller than control littermates (Fig. 5A). *Foxi3* cKO mice had a sparse coat that was visible as soon as the hairs first protruded from the skin surface in control littermates. However, the coat appeared denser and thus the phenotype was less severe than in *Foxi3* KO skin grafts, possibly owing to the mixed background of *Foxi3* cKO mice. In some mutant mice, the phenotype visibly progressed with age (Fig. 5A, S6A). The fur of *Foxi3* cKO mice contained all 4 hair types in a normal ratio (Fig. S7A; data not shown), and the external hair structure was not affected either (Fig. 5B).

We next examined whether *Foxi3* ablation would affect progression of HFs through the first synchronized cycle. At postnatal day 10 (P10), a large number of *Foxi3* cKO follicles displayed morphological abnormalities, such as cysts (Fig. 5C). Many *Foxi3* cKO HFs were delayed in proceeding through catagen and telogen, compared to controls (Fig. 5D, 5E, S6). At the first telogen, many mutant follicles displayed abnormal morphology: an absence of a clearly discernible bulge and HG, as well as enlarged sebaceous glands (Fig. 5E). When controls progressed to anagen, many *Foxi3* cKO follicles had not yet completed catagen and failed to regrow (Fig. 5F).

Progressive depletion of SC niche in Foxi3 cKO mice

To identify the defect behind poor anagen entry caused by *Foxi3* deletion, we studied expression of SC markers at two different stages: at the first telogen, and at the age of 1 year, i.e. after several cycles of regeneration. Already at the first telogen, many *Foxi3* cKO HFs displayed depletion of SC niche, i.e. bulge and HG, as shown by decreased expression of Sox9 and Lhx2 (Fig. 6A, 6B). Quantification revealed significantly fewer Lhx2+ HFs in *Foxi3* cKO mice (Fig. 6C). The number of Lhx2+ cells per bulge was also less in *Foxi3* cKO

at first telogen (Fig. 6D). Lef1+ HG/early TA cells, which are indicative of activated Wnt signaling, were largely absent from affected *Foxi3* cKO HFs at anagen onset, and P-cadherin was also reduced (Fig. 6E). At one year of age, the amount of HFs with abnormal morphology (with cysts and enlarged sebaceous glands) was increased compared to the first telogen (Fig. 6F), a finding that is indicative of exhaustion of SC reservoirs. This was confirmed by quantification of Lhx2+ follicles: *Foxi3* cKO had fewer Lhx2+ follicles at 1 year of age compared to the first telogen (Fig. 6C, 6G) confirming a progressive phenotype suggested by macroscopic inspection of *Foxi3* cKO mice (Figs. 5A, S6A). Thus, although expression of Foxi3 is exclusively restricted to the HG, its absence leads to gradual loss of bulge SCs.

Foxi3 is required for the hair follicle SC activation to initiate hair regeneration

To assess the function of Foxi3 further, we used a depilation-induced SC activation model. Hairs were depilated at the second telogen to induce synchronized anagen entry and hair regeneration. Upon hair plucking, *Foxi3* cKO mice regrew hairs more slowly than controls, and their coats remained very sparse when compared to pre-plucking state (Fig. 7A, S7C). It was previously shown that similarly to spontaneous anagen, during depilation-induced anagen, HG cells proliferate already at day 1 post plucking (dpp1), whereas bulge SC proliferation is only observed at dpp2, but even then at reduced levels compared to HG [11]. At dpp2, BrdU incorporation revealed activated proliferation in the lower growing portion of HFs, indicating that control HFs had entered a new hair cycle, while *Foxi3* cKO HFs showed a significant decrease in SC activation (Fig. 7B, 7C). Even at dpp15, when HFs had reached full anagen in control mice, the majority of *Foxi3* cKO HFs remained growth arrested (Fig. 7D).

Foxi3 is involved in Shh-based feedback loop activating bulge SCs at telogen-anagen transition

The activating cue for bulge SC proliferation is Shh produced by TA cells [11]. We analyzed *Shh* expression in *Foxi3* cKO HFs at the onset of the first anagen and after depilation. Most *Foxi3* cKO HFs were negative for *Shh* expression at anagen onset (Fig. 7E). Similarly after depilation, the majority of *Foxi3* cKO HFs were negative for *Shh* and failed to initiate anagen at dpp2 (Fig. S7D). These data indicate a critical role for Foxi3 in initiation of *Shh* expression in early TA cells. Why *Foxi3* deficiency precludes *Shh* expression in HG/TA cells at the onset of anagen, but not during morphogenesis (Fig. S4D, S4D) is currently not known.

To further delineate the function of Foxi3 in HG activation, we tried to inducibly delete *Foxi3* using K14-Cre^{ERT} mice, but obtained poor *Foxi3* deletion (data not shown). We next generated *Foxi3*$^{null/floxed}$;Lgr5Cre^{ERT2} mice (hereafter *Foxi3* icKO) to ablate *Foxi3* specifically in the HG during the second telogen by tamoxifen injections (Fig. S7E). Depilated *Foxi3* icKO grew hairs back normally, without delay or other obvious defects (Fig. S7F). However, more precise analysis of the *Foxi3* icKO skins showed again an inefficient deletion of *Foxi3* (Fig. S7G). We analyzed dpp2 HFs from 4 Foxi3 icKO mice and found that 0/19 Foxi3-negative HFs (confirmed by Foxi3 immunostaining on serial sections) initiated growth while 100/100 Foxi3+ HFs proceeded to anagen (Fig. S7G; and

data not shown), implying a specific involvement of Foxi3 in HG activation and HF regeneration.

DISCUSSION

In this study we tested the function of the Foxi3 transcription factor, mutated in three hairless dog breeds [40], in hair follicle development and turnover using mouse models. Analysis of Foxi3 mRNA and protein *in situ* uncovered a highly dynamic expression pattern during HF morphogenesis and cycling, and we identify Foxi3 as a novel marker of the secondary HG. Foxi3 is expressed in all hair follicle types and all follicle types were affected by loss of Foxi3. We previously identified Foxi3 as a target gene of Eda [39], a pathway essential for primary hair follicle morphogenesis only. Instead, Foxi3 deficiency impairs all follicle types suggesting that Foxi3 has also functions unrelated to Eda signaling. We show that loss of Foxi3 compromises several aspects of HF development and regeneration: downgrowth during embryogenesis, specification of SCs, maintenance of HF architecture, catagen onset, and activation/maintenance of SCs (Fig. 7F). However, although Foxi3 is transiently expressed in hair shaft precursors we found no evidence for a function in hair shaft formation. Only a few hairs formed in *Foxi3* KO skin grafts and *Foxi3* cKO mutants had a sparse coat. Hair shafts that did form had a normal appearance suggesting that absence of hair is a secondary phenotype due to defects in morphogenesis and SCs.

Foxi3 is required for hair follicle downgrowth

We show here that HF downgrowth is impaired from the earliest (germ) stage onward in *Foxi3* KO embryos. This phenotype resembles, but is milder than that of *Shh* null embryos [35,36], suggesting a link between the two pathways. However, *Foxi3* expression was unaltered in *Shh* embryos (data not shown), and loss of *Foxi3* did not disturb Shh, or any other major signaling pathway involved in progression of HF morphogenesis. Instead, microarray profiling of E15.5 skin epithelia implicated several SC signature genes downstream of Foxi3 including *Nfatc1, Runx1, Klf4*, and *Lhx2*. Lhx2 is expressed in HFs already at the placode stage [22,56], but its transcriptional regulation is poorly understood.

Lhx2 was undetectable in *Foxi3* KO HFs at E15.5, but its expression reappeared later indicating involvement of additional factors in its regulation, Shh being one candidate [22]. During early stages of HF development Lhx2 is enriched in cells of the leading front of invaginating HFs. It has been proposed that embryonic HF morphogenesis is driven by the Lhx2+ cell population, but being replaced postnatally by progeny of the $Sox9^{+}$ early bulge cells, which in turn contribute little to embryonic growth [19]. As loss of *Foxi3* leads to a similar embryonic phenotype as Lhx2 deficiency [22,23,56], and cell proliferation was reduced in Foxi3 KOs specifically at germ stage, we propose that the embryonic *Foxi3* KO downgrowth defect is largely due to delayed onset of Lhx2 expression with possible contribution of Runx1, which is also implicated in embryonic HF downgrowth [57].

Foxi3 regulates SC specification

The reduced expression of several SC genes in E15.5 *Foxi3* KO epithelium prompted us to analyze bulge formation in more detail. Although expression of Sox9, the master regulator

of SC specification [19,20,30,58] was apparently unaltered in *Foxi3* KO embryonic skin (no changes in mRNA levels assessed by qRT-PCR at E15.5 either; data not shown), we noticed significantly reduced number of HFs expressing Nfatc1 and K15 prior to birth, indicating defects in pre-bulge formation. Nfatc1 and Runx1 are individually dispensable for SC specification [15,17,57]. Interestingly, a recent study revealed that super-enhancers underlie the lineage commitment of HF SCs by regulating a repertoire of SC signature genes [58]. Super-enhancers were shown to display clusters of binding sites occupied by ≥5 HF SC transcription factors including Sox9, Lhx2, and Nfatc1. As these binding motifs enable cooperative binding, it is possible that simultaneous downregulation of more than one of these factors may significantly impair the expression of several stemness genes and thereby compromise SC specification and activation. A fault in SC specification may also explain the notable downgrowth defect of the grafted Foxi3 KO skin, as the early bulge cells are needed to maintain the pool of TA cells to complete post-natal morphogenesis [19].

The HFs in early postnatal *Foxi3* cKO mice displayed morphological abnormalities, failed to enter the first catagen synchronously, and had cysts and/or enlarged sebaceous glands by the first telogen. Thus, Foxi3 is not only required to establish the SC compartment and complete morphogenesis, but is involved also in catagen. Defects in executing catagen in turn may compromise formation of the secondary hair germ. A bulge defect, likely stemming from the earlier failure to establish the pre-bulge was also evident: Sox9 expression was diminished, and the number of Lhx2+ HFs, as well as SCs per HF, was significantly reduced in *Foxi3* cKO mice at first telogen.

Loss of Foxi3 compromises SC activation and maintenance

Both developmental and depilation-driven HF regeneration was impaired in *Foxi3* cKO mice indicating a critical function for Foxi3 in SC activation. Several studies show a key role for the Wnt/β-cat pathway in HG activation [10,25,59], and Shh expression by HG progenitors in turn is necessary for bulge SC activation [11]. Foxi3 is exclusively expressed in the HG, not in the bulge. Therefore it is likely that a failure in HG activation impairs bulge activation in *Foxi3* cKO HFs. Accordingly, we detected few Lef1+ and *Shh+* HFs at anagen onset indicating that Foxi3 is essential for Wnt pathway activation and expansion of TA cells. The exact mechanism whereby Foxi3 promotes Wnt signaling is currently unclear but may involve Runx1 which was shown to enhance Wnt signaling [57]. Runx1 is enriched in the HG and its epithelial deletion delays anagen onset by weeks despite the presence of SCs at normal numbers [17,60].

A recent RNA-seq profiling study showed that *Foxi3* expression is highly induced in telogen SCs/TA cells upon deletion of Bmpr1a [34], a condition instigating SC activation [30,34]. To distinguish between the role of Foxi3 in SC specification and postnatal SC activation/maintenance, we conditionally ablated *Foxi3* during the second telogen. Unfortunately, despite our best efforts, the deletion efficiency was not sufficient to draw reliable conclusions. Therefore we cannot fully exclude the possibility that poor HF regeneration is secondary to the developmental function of Foxi3. However, the progressive loss of SCs in aging *Foxi3* cKO mice is suggestive of an independent function in HF homeostasis. This is also in line with recent findings showing the importance of HG in the long-term regenerative

capacity of the bulge: Shh emanating from HG/TA cells is essential for self-renewal of SCs to replenish the niche [11]. Further, as Foxi3 expression is turned on in catagenic HFs, it may also be involved in homing and turnover of new bulge/HG cells.

CONCLUSIONS

In summary, our study has revealed several functions for Foxi3 in hair follicle biology, in particular in the establishment and activation of the stem cell niche. Of note, Foxi3 was undetectable in the incipient stem cell niche (embryonic pre-bulge) and was expressed in the Sox9+ stem cell precursor population only at placode/early germ stage suggesting that critical stem cell fate decisions take place earlier than previously recognized, prior to the morphologically discernible SC niche. Further, our results identify Foxi3 as a novel, secondary hair germ resident mediator of dermal papilla-derived cues essential for activation of quiescent bulge stem cells.

Supplementary Material

Refer to Web version on PubMed Central for supplementary material.

Acknowledgments

We thank Irma Thesleff for support and discussions, and Merja Mäkinen, Riikka Santalahti, Maria Sanz-Navarro, Raija Savolainen, and Nina Tiusanen for technical assistance. This work was financially supported by Swiss National Science Foundation Sinergia grant CRSI33_125459, the Academy of Finland, Sigrid Jusélius Foundation, Jane and Aatos Erkko Foundation, the Ella and Georg Ehrnrooth Foundation, and RO1 DC013072 and RO3 DC007349.

REFERENCES

1. Biggs LC, Mikkola ML, et al. Early inductive events in ectodermal appendage morphogenesis. Semin.Cell Dev.Biol. 2014; 25–26:11–21.
2. Sennett R, Rendl M, et al. Mesenchymal-epithelial interactions during hair follicle morphogenesis and cycling. Semin.Cell Dev.Biol. 2012; 23:917–927. [PubMed: 22960356]
3. Hsu YC, Pasolli HA, Fuchs E. Dynamics between stem cells, niche, and progeny in the hair follicle. Cell. 2011; 144:92–105. [PubMed: 21215372]
4. Legue E, Nicolas JF. Hair follicle renewal: organization of stem cells in the matrix and the role of stereotyped lineages and behaviors. Development. 2005; 132:4143–4154. [PubMed: 16107474]
5. Paus R, Muller-Rover S, Van Der Veen C, et al. A comprehensive guide for the recognition and classification of distinct stages of hair follicle morphogenesis. J.Invest.Dermatol. 1999; 113:523–532. [PubMed: 10504436]
6. Rompolas P, Greco V. Stem cell dynamics in the hair follicle niche. Semin.Cell Dev.Biol. 2014; 25–26:34–42.
7. Cotsarelis G, Sun TT, Lavker RM. Label-retaining cells reside in the bulge area of pilosebaceous unit: implications for follicular stem cells, hair cycle, and skin carcinogenesis. Cell. 1990; 61:1329–1337. [PubMed: 2364430]
8. Morgan BA. The dermal papilla: an instructive niche for epithelial stem and progenitor cells in development and regeneration of the hair follicle. Cold Spring Harb Perspect.Med. 2014; 4:a015180. [PubMed: 24985131]
9. Rompolas P, Mesa KR, Greco Vl. Spatial organization within a niche as a determinant of stem-cell fate. Nature. 2013; 502:513–518. [PubMed: 24097351]
10. Greco V, Chen T, Rendl M, et al. A two-step mechanism for stem cell activation during hair regeneration. Cell.Stem Cell. 2009; 4:155–169. [PubMed: 19200804]

11. Hsu YC, Li L, Fuchs E. Transit-amplifying cells orchestrate stem cell activity and tissue regeneration. Cell. 2014; 157:935–949. [PubMed: 24813615]
12. Goldstein J, Horsley V. Home sweet home: skin stem cell niches. Cell Mol.Life Sci. 2012; 69:2573–2582. [PubMed: 22410738]
13. Schepeler T, Page ME, Jensen KB. Heterogeneity and plasticity of epidermal stem cells. Development. 2014; 141:2559–2567. [PubMed: 24961797]
14. Trempus CS, Morris RJ, Bortner CD, et al. Enrichment for living murine keratinocytes from the hair follicle bulge with the cell surface marker CD34. J.Invest.Dermatol. 2003; 120:501–511. [PubMed: 12648211]
15. Horsley V, Aliprantis AO, Polak L, et al. NFATc1 balances quiescence and proliferation of skin stem cells. Cell. 2008; 132:299–310. [PubMed: 18243104]
16. Muller-Rover S, Tokura Y, Welker P, et al. E- and P-cadherin expression during murine hair follicle morphogenesis and cycling. Exp.Dermatol. 1999; 8:237–246. [PubMed: 10439220]
17. Osorio KM, Lee SE, McDermitt DJ, et al. Runx1 modulates developmental, but not injury-driven, hair follicle stem cell activation. Development. 2008; 135:1059–1068. [PubMed: 18256199]
18. Levy V, Lindon C, Harfe BD, et al. Distinct stem cell populations regenerate the follicle and interfollicular epidermis. Dev.Cell. 2005; 9:855–861. [PubMed: 16326396]
19. Nowak JA, Polak L, Pasolli HA, et al. Hair follicle stem cells are specified and function in early skin morphogenesis. Cell.Stem Cell. 2008; 3:33–43. [PubMed: 18593557]
20. Vidal VP, Chaboissier MC, Lutzkendorf S, et al. Sox9 is essential for outer root sheath differentiation and the formation of the hair stem cell compartment. Curr.Biol. 2005; 15:1340–1351. [PubMed: 16085486]
21. Kadaja M, Keyes BE, Lin M, et al. SOX9: a stem cell transcriptional regulator of secreted niche signaling factors. Genes Dev. 2014; 28:328–341. [PubMed: 24532713]
22. Rhee H, Polak L, Fuchs E. Lhx2 maintains stem cell character in hair follicles. Science. 2006; 312:1946–1949. [PubMed: 16809539]
23. Mardaryev AN, Meier N, Poterlowicz K, et al. Lhx2 differentially regulates Sox9, Tcf4 and Lgr5 in hair follicle stem cells to promote epidermal regeneration after injury. Development. 2011; 138:4843–4852. [PubMed: 22028024]
24. Nguyen H, Rendl M, Fuchs E. Tcf3 governs stem cell features and represses cell fate determination in skin. Cell. 2006; 127:171–183. [PubMed: 17018284]
25. Lien WH, Polak L, Lin M, et al. In vivo transcriptional governance of hair follicle stem cells by canonical Wnt regulators. Nat.Cell Biol. 2014; 16:179–190. [PubMed: 24463605]
26. Andl T, Reddy ST, Gaddapara T, et al. WNT signals are required for the initiation of hair follicle development. Dev.Cell. 2002; 2:643–653. [PubMed: 12015971]
27. Botchkarev VA, Botchkareva NV, Roth W, et al. Noggin is a mesenchymally derived stimulator of hair-follicle induction. Nat.Cell Biol. 1999; 1:158–164. [PubMed: 10559902]
28. Pummila M, Fliniaux I, Jaatinen R, et al. Ectodysplasin has a dual role in ectodermal organogenesis: inhibition of Bmp activity and induction of Shh expression. Development. 2007; 134:117–125. [PubMed: 17164417]
29. Jamora C, DasGupta R, Kocieniewski P, et al. Links between signal transduction, transcription and adhesion in epithelial bud development. Nature. 2003; 422:317–322. [PubMed: 12646922]
30. Kandyba E, Leung Y, Chen YB, et al. Competitive balance of intrabulge BMP/Wnt signaling reveals a robust gene network ruling stem cell homeostasis and cyclic activation. Proc.Natl.Acad.Sci.U.S.A. 2013; 110:1351–1356. [PubMed: 23292934]
31. Lowry WE, Blanpain C, Nowak JA, et al. Defining the impact of beta-catenin/Tcf transactivation on epithelial stem cells. Genes Dev. 2005; 19:1596–1611. [PubMed: 15961525]
32. Plikus MV, Mayer JA, de la Cruz D, et al. Cyclic dermal BMP signalling regulates stem cell activation during hair regeneration. Nature. 2008; 451:340–344. [PubMed: 18202659]
33. Van Mater D, Kolligs FT, Dlugosz AA, et al. Transient activation of beta -catenin signaling in cutaneous keratinocytes is sufficient to trigger the active growth phase of the hair cycle in mice. Genes Dev. 2003; 17:1219–1224. [PubMed: 12756226]

34. Genander M, Cook PJ, Ramskold D, et al. BMP signaling and its pSMAD1/5 target genes differentially regulate hair follicle stem cell lineages. Cell.Stem Cell. 2014; 15:619–633. [PubMed: 25312496]
35. St-Jacques B, Dassule HR, Karavanova I, et al. Sonic hedgehog signaling is essential for hair development. Curr.Biol. 1998; 8:1058–1068. [PubMed: 9768360]
36. Chiang C, Swan RZ, Grachtchouk M, et al. Essential role for Sonic hedgehog during hair follicle morphogenesis. Dev.Biol. 1999; 205:1–9. [PubMed: 9882493]
37. Petiot A, Conti FJ, Grose R, et al. A crucial role for Fgfr2-IIIb signalling in epidermal development and hair follicle patterning. Development. 2003; 130:5493–5501. [PubMed: 14530295]
38. Mikkola ML. Molecular aspects of hypohidrotic ectodermal dysplasia. Am.J.Med.Genet.A. 2009; 149A:2031–2036. [PubMed: 19681132]
39. Shirokova V, Jussila M, Hytonen MK, et al. Expression of Foxi3 is regulated by ectodysplasin in skin appendage placodes. Dev.Dyn. 2013; 242:593–603. [PubMed: 23441037]
40. Drogemuller C, Karlsson EK, Hytonen MK, et al. A mutation in hairless dogs implicates FOXI3 in ectodermal development. Science. 2008; 321:1462. [PubMed: 18787161]
41. Wiener DJ, Gurtner C, Panakova L, et al. Clinical and histological characterization of hair coat and glandular tissue of Chinese crested dogs. Vet.Dermatol. 2013; 24:274–e62. [PubMed: 23413772]
42. Bianchi N, Depianto D, McGowan K, et al. Exploiting the keratin 17 gene promoter to visualize live cells in epithelial appendages of mice. Mol.Cell.Biol. 2005; 25:7249–7259. [PubMed: 16055733]
43. Bhakar AL, Tannis LL, Zeindler C, et al. Constitutive nuclear factor-kappa B activity is required for central neuron survival. J.Neurosci. 2002; 22:8466–8475. [PubMed: 12351721]
44. Maretto S, Cordenonsi M, Dupont S, et al. Mapping Wnt/beta-catenin signaling during mouse development and in colorectal tumors. Proc.Natl.Acad.Sci.U.S.A. 2003; 100:3299–3304. [PubMed: 12626757]
45. Edlund RK, Ohyama T, Kantarci H, et al. Foxi transcription factors promote pharyngeal arch development by regulating formation of FGF signaling centers. Dev.Biol. 2014; 390:1–13. [PubMed: 24650709]
46. Andl T, Ahn K, Kairo A, et al. Epithelial Bmpr1a regulates differentiation and proliferation in postnatal hair follicles and is essential for tooth development. Development. 2004; 131:2257–2268. [PubMed: 15102710]
47. Huelsken J, Vogel R, Erdmann B, et al. beta-Catenin controls hair follicle morphogenesis and stem cell differentiation in the skin. Cell. 2001; 105:533–545. [PubMed: 11371349]
48. Narhi K, Jarvinen E, Birchmeier W, et al. Sustained epithelial beta-catenin activity induces precocious hair development but disrupts hair follicle down-growth and hair shaft formation. Development. 2008; 135:1019–1028. [PubMed: 18256193]
49. Ohyama T, Groves AK. Expression of mouse Foxi class genes in early craniofacial development. Dev.Dyn. 2004; 231:640–646. [PubMed: 15376323]
50. Vaahtokari A, Aberg T, Jernvall J, et al. The enamel knot as a signaling center in the developing mouse tooth. Mech.Dev. 1996; 54:39–43. [PubMed: 8808404]
51. Zhang X, Ibrahimi OA, Olsen SK, et al. Receptor specificity of the fibroblast growth factor family. The complete mammalian FGF family. J.Biol.Chem. 2006; 281:15694–15700. [PubMed: 16597617]
52. Li J, Zheng H, Wang J, et al. Expression of Kruppel-like factor KLF4 in mouse hair follicle stem cells contributes to cutaneous wound healing. PLoS One. 2012; 7:e39663. [PubMed: 22745808]
53. Fliniaux I, Mikkola ML, Lefebvre S, et al. Identification of dkk4 as a target of Eda-A1/Edar pathway reveals an unexpected role of ectodysplasin as inhibitor of Wnt signalling in ectodermal placodes. Dev Biol. 2008; 320:60–71. [PubMed: 18508042]
54. Kazantseva A, Goltsov A, Zinchenko R, et al. Human hair growth deficiency is linked to a genetic defect in the phospholipase gene LIPH. Science. 2006; 314:982–985. [PubMed: 17095700]
55. Panteleyev AA, Botchkareva NV, Sundberg JP, et al. The role of the hairless (hr) gene in the regulation of hair follicle catagen transformation. Am.J.Pathol. 1999; 155:159–171. [PubMed: 10393848]

56. Tornqvist G, Sandberg A, Hagglund AC, et al. Cyclic expression of lhx2 regulates hair formation. PLoS Genet. 2010; 6:e1000904. [PubMed: 20386748]

57. Osorio KM, Lilja KC, Tumbar T. Runx1 modulates adult hair follicle stem cell emergence and maintenance from distinct embryonic skin compartments. J.Cell Biol. 2011; 193:235–250. [PubMed: 21464233]

58. Adam RC, Yang H, Rockowitz S, et al. Pioneer factors govern super-enhancer dynamics in stem cell plasticity and lineage choice. Nature. 2015; 521:366–370. [PubMed: 25799994]

59. Choi YS, Zhang Y, Xu M, et al. Distinct functions for Wnt/beta-catenin in hair follicle stem cell proliferation and survival and interfollicular epidermal homeostasis. Cell.Stem Cell. 2013; 13:720–733. [PubMed: 24315444]

60. Hoi CS, Lee SE, Lu SY, et al. Runx1 directly promotes proliferation of hair follicle stem cells and epithelial tumor formation in mouse skin. Mol.Cell.Biol. 2010; 30:2518–2536. [PubMed: 20308320]

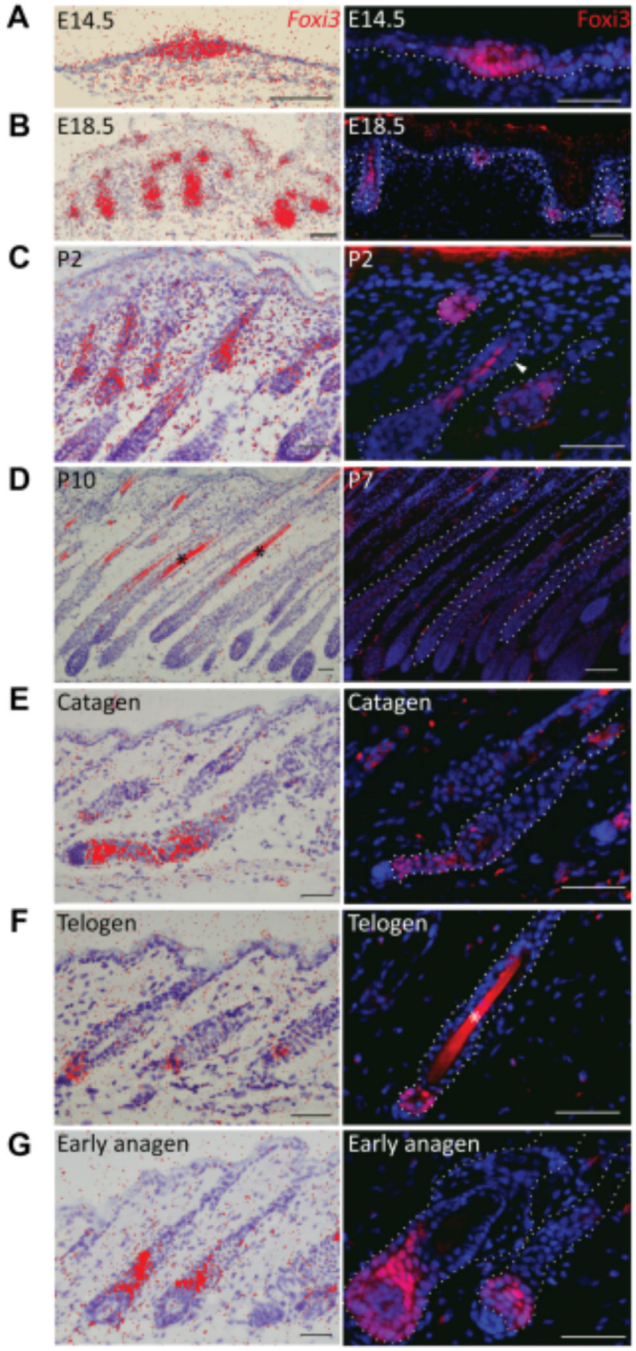

Figure 1.

Foxi3 displays a dynamic expression pattern during hair morphogenesis and cycling. Radioactive in situ hybridization (left column) and immunostaining (right column) for Foxi3 at indicated stages of hair morphogenesis and cycle. (A): Foxi3 was detected in epithelial cells of the hair placode. (B, C): In more advanced follicles, Foxi3 was detected in the lower part of the hair peg and later only in cells in the center of the follicle above the matrix likely representing the hair shaft precursors. Note absence of protein expression in the upper part of the outer root sheath (pre-bulge) (arrowhead). (D): Foxi3 was no longer detected in fully

formed hair follicles. (E): Foxi3 reappeared at catagen, in the cells of the regressing epithelial strand. (F): At telogen, Foxi3 was restricted exclusively to the cells of the hair germ between bulge and dermal papilla. (G): At the onset of anagen Foxi3 expression expanded into the growing portion of the follicle. Unspecific staining observed in the hair shaft is indicated by a star.

Scale bar=50 μm. Abbreviations: E=embryonic day; P=postnatal day.

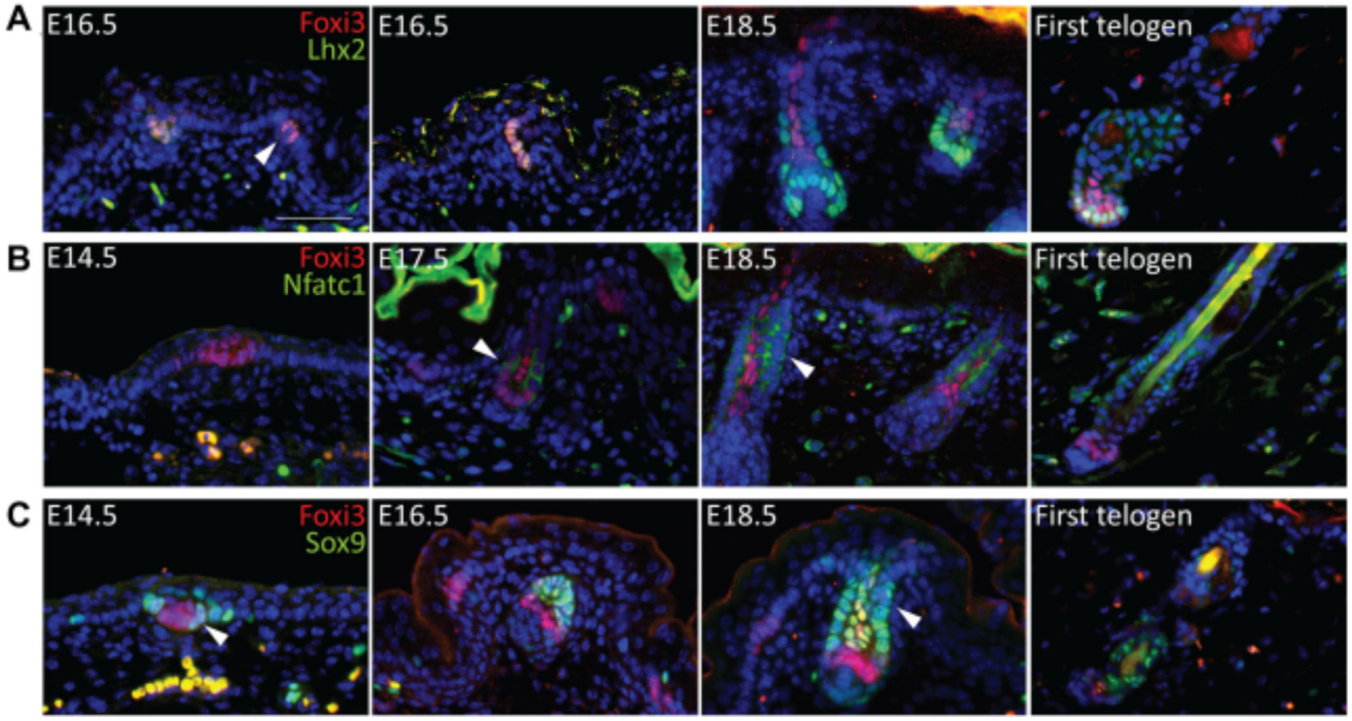

Figure 2.

Foxi3 expression colocalizes with stem cell markers only at the beginning of hair morphogenesis and later in telogen follicle secondary hair germs. Co-localization of Foxi3 (red) with stem cell markers Lhx2, Nfatc1, and Sox9 (green) at different stages of hair morphogenesis and at the first telogen was analysed by double immunostaining. (A): Foxi3 was co-expressed with Lhx2 in hair placodes and in the leading front of the growing hair follicle. At advanced stages of development, Foxi3+ cells in the center were negative for Lhx2. At telogen, Foxi3+ cells in the hair germ also expressed Lhx2. (B): Nfatc1 was undetectable at the placode stage, but co-localized with Foxi3 at the hair peg stage (arrowhead). In advanced hair follicles (E18.5), Foxi3+ cells in the center were negative for Nfatc1, which was expressed in the pre-bulge region (arrowhead). At telogen, Nfatc1marked the quiescent SCs of the upper bulge and was not co-expressed with Foxi3 in the hair germ. (C): Some cells of the placode were positive for both Foxi3 and Sox9. At the hair germ stage, Sox9 did not co-localize with Foxi3+ cells at the leading front, but a small number of cells positive for both Foxi3 and Sox9 appeared in the middle of the growing hair peg. In addition, Sox9 was detected in the upper part of the follicle (arrowhead). At telogen, Foxi3+ cells in the hair germ were also positive for Sox9, but the latter was expressed also in the bulge. Scale bar=50 μm. Abbreviations: E=embryonic day; P=postnatal day.

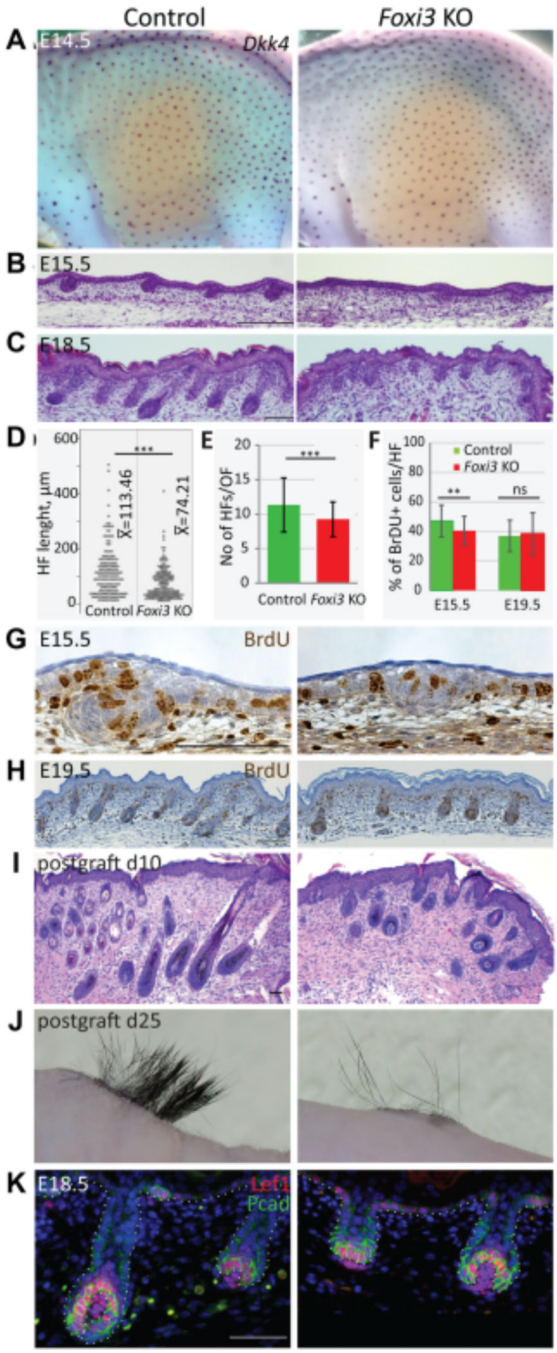

Figure 3.

Normal patterning but impaired downgrowth of hair follicles in *Foxi3* KO embryos. (A): Primary hair follicle formation was not affected in *Foxi3* KO, whole mount in situ hybridization using a probe specific for placode marker *Dkk4*. (B): Impaired invagination of hair buds in *Foxi3* KO was detected in hematoxylin and eosin stained histological sections of E15.5 back skins. (C): The downgrowth defect of *Foxi3* KO hair follicles was evident also at E18.5. (D): Dot plots of hair follicle length at late embryogenesis measured from *Foxi3* KO (N=183 follicles from 5 embryos), and control littermates (N=178 follicles from 4 embryos);

p=4.27 E-5. (E): Quantification of the number of hair follicles per optic field revealed decreased number of hair follicles in *Foxi3* KO (n=62 OFs from 4 embryos; 575 hair follicles were scored) compared to control littermates (n=59 OFs from 4 embryos; 669 hair follicles were scored) at late embryogenesis; p=0.00093. (F): Quantification of percentage of BrdU+ cells per hair follicle at E15.5 showed decreased proliferation in Foxi3 KO (n=4, 48 hair follicles, 1271 cells scored) compared to control littermates (n=4, 48 hair follicles, 1610 cells scored), p=0.0026; no differences were found at E19.5 between Foxi3 KO (n=3 embryos, 82 HFs, 3217 cells scored) and control littermates (n=3 embryos, 70 hair follicles, 3079 cells scored). (G, H): BrdU staining in Foxi3 KO and littermate control embryos at E15.5 (G) and at E19.5 (H). (I): Impaired HF downgrowth in skin grafts of E18.5 Foxi3 KO (n= 5) compared to control explants (n=6) transplanted onto back skin of immunocompromised Nude mice, 10 days post grafting. (J): Macroscopic pictures at 25 days post grafting. (K): Expression of Lef1 was not affected in *Foxi3* KO hair follicles at E18.5. Scale bar=50 μm. Data are shown as mean±SD. P-values were estimated using unpaired two-tailed Student t-test. Abbreviations: E=embryonic day; OF=optic field; HF=hair follicle; ns=non-significant (p>0.05).

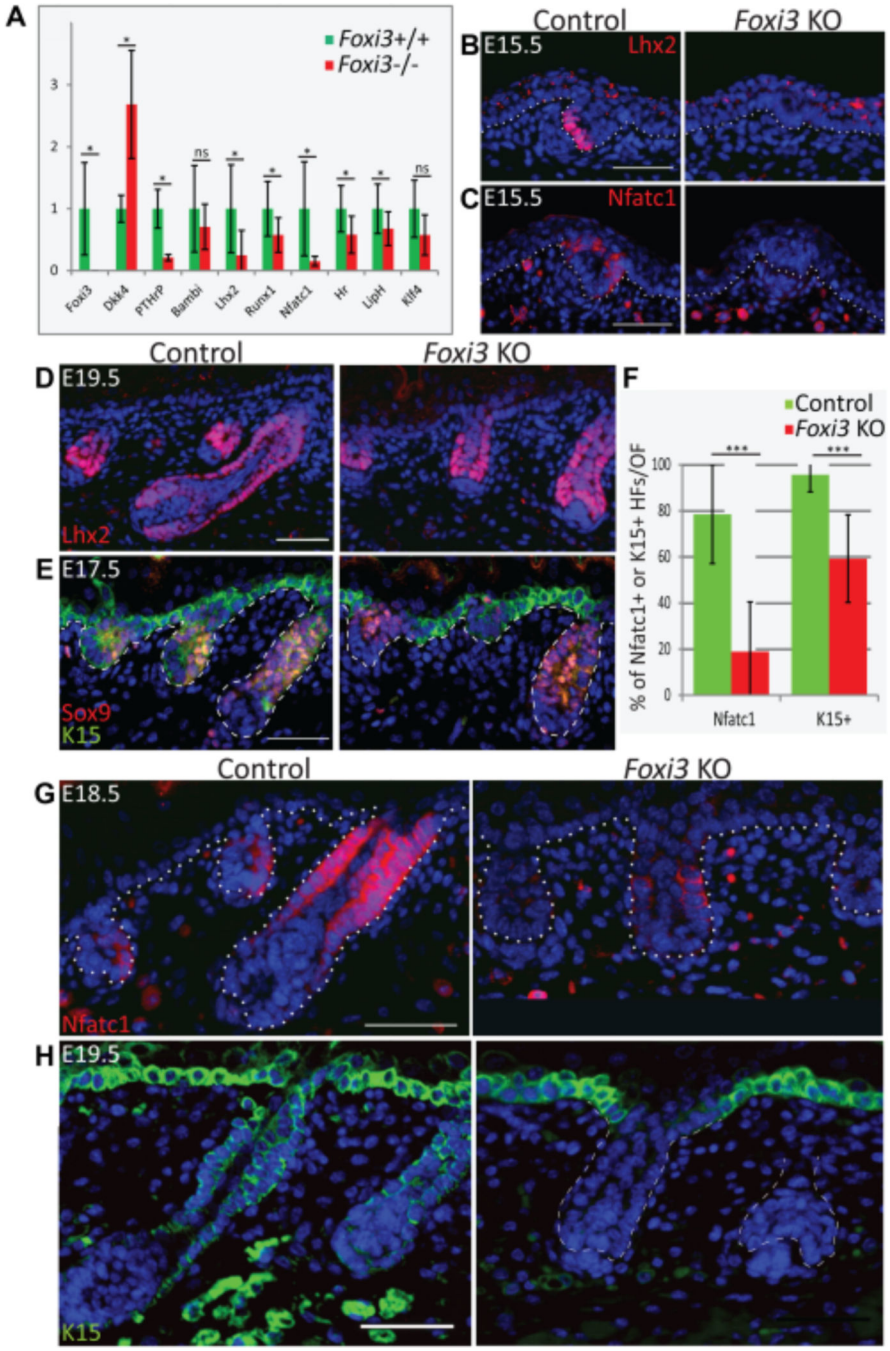

Figure 4.

Several SC signature genes were downregulated in *Foxi3* KO hair follicles during morphogenesis. (A): qRT-PCR analysis of indicated genes (selected based on differential expression in the microarray) in8ä

ä E15.5 epithelia isolated from *Foxi3* KO and wild-type littermates. (n=6 per genotype; *p<0.05, related-samples Wilcoxon signed ranked test, IBM SPSS Statistics). (B, C): Expression of Lhx2 (B) or Nfatc1(C) was not detected in *Foxi3* KO hair follicles at E15.5. (D, E): At later stages, *Foxi3* KO hair follicles showed relatively normal staining for Lhx2

(D) and Sox9 (E). (F–H): In contrast, Nfatc1 and K15 were downregulated in *Foxi3* KO embryos at E18.5-E19.5. However, K15 staining in the basal epidermis was indistinguishable in control and *Foxi3* KO embryos. (F): Quantification of percent of Nfatc1+ and K15+ hair follicles per optic field in *Foxi3* KO and control littermates at late morphogenesis. Nfatc1: *Foxi3* KO (n=182 OFs from 3 embryos; 760 hair follicles were scored) and control littermates (n=164 OFs from 3 embryos; 881 hair follicles were scored); p=2.21 E-82. K15: *Foxi3* KO (n=47 OFs from 3 embryos; 410 hair follicles were scored) and control littermates (n=42 OFs from 2 embryos; 502 hair follicles were scored), p=2.67 E-19. Data are shown as mean±SD. P-values were estimated using unpaired two-tailed Student t-test. (G, H): Representative images of Nfatc1 and K15 staining at late embryogenesis in control and *Foxi3* KO hair follicles.
Scale bar=50 μm. Abbreviations: E=embryonic day; OF=optic field; ns=non-significant ($p>0.05$).

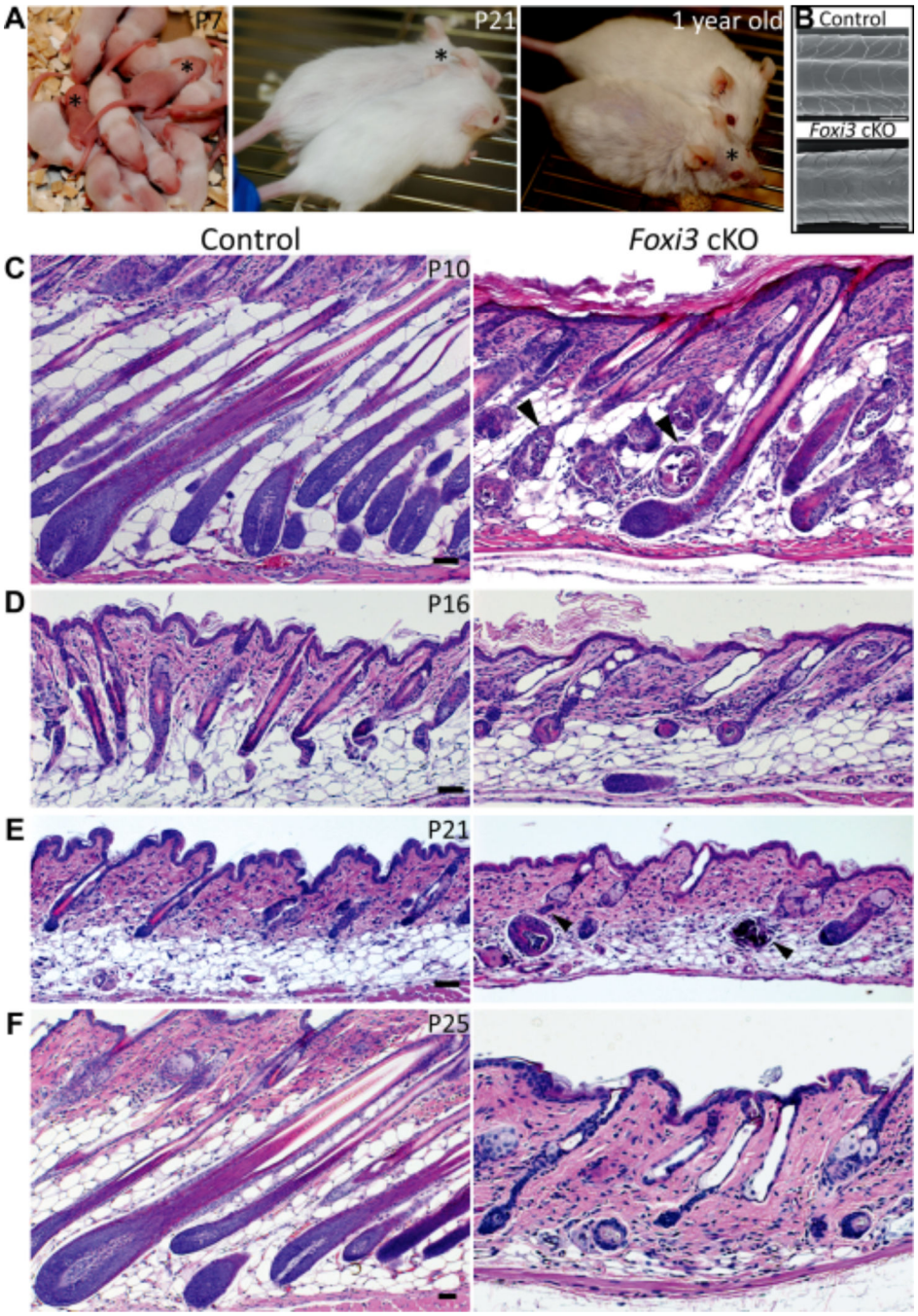

Figure 5.

Foxi3 cKO mice show sparse fur and asynchronous hair cycle. (A): *Foxi3* cKO mice (marked with *) displayed a sparse coat by P7. The phenotype was stable throughout life and was further exacerbated in older mice (1 year old). (B): Scanning electron microscopy image of an awl hair shaft of control and *Foxi3* cKO littermates at 2.5 months of age showed no changes in external hair structure. (C–F): Hematoxylin and eosin stained histological sections of control and *Foxi3* cKO back skin at indicated time points. (C): At P10, a large fraction of *Foxi3* cKO follicles displayed morphological abnormalities (arrowheads). (D):

Many *Foxi3* cKO hair follicles were delayed in proceeding through catagen. (E): At first telogen, a big amount of *Foxi3* cKO follicles displayed abnormal morphology, including absence of clearly discernible bulge and HG (arrowheads), enlarged sebaceous glands, widened hair channels, and cyst formation. (F): At P25, control follicles had proceeded to first anagen, whereas many *Foxi3* cKO follicles had not yet completed catagen and failed to initiate a new growth phase.

Scale bar=20 μm (B), 50 μm (C–F). Abbreviations: P=postnatal day.

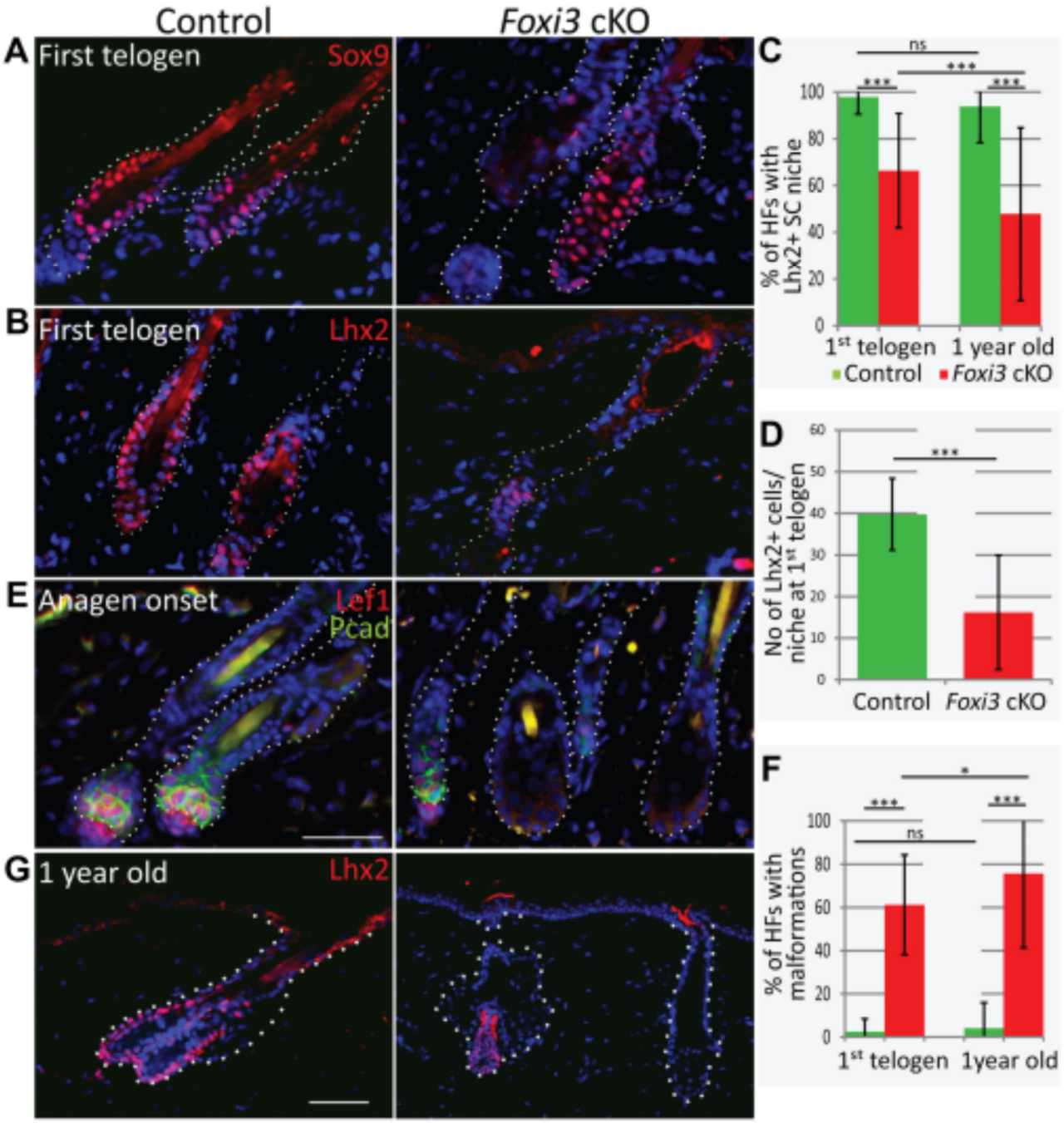

Figure 6.

Stem cells are progressively depleted in *Foxi3* cKO hair follicles. (A, B): Reduced number of cells positive for stem cell markers Sox9 (A) and Lhx2 (B) in *Foxi3* cKO hair follicles at first telogen, P20. (C): Quantification of percent of hair follicles which contained at least some Lhx2+ cells at the first telogen and at 1 year of age showed a progressive phenotype. At first telogen: control littermates (n=47 OFs from 3 mice; 296 follicles were scored) and *Foxi3* cKO (n=40 OFs from 3 mice; 257 hair follicles were scored). At 1 year of age: control (n=61OFs from 3 mice; 142 hair follicles were scored) and *Foxi3* cKO (n=61 OFs from 3

mice; 147 hair follicles); p (Control$^{1st\ telogen}$ vs. *Foxi3* cKO$^{1st\ telogen}$)=5.0 E-10; p (control$^{1y\ old}$ vs. *Foxi3* cKO$^{1y\ old}$)=8.7 E-14; p (*Foxi3* cKO$^{1st\ telogen}$ vs. *Foxi3* cKO$^{1y\ old}$)=0.0031. (D): Quantification of Lhx2+ cells per SC niche (bulge and HG) in control (n=16 follicles from 3 mice, 636 cells were scored) and per SC niche residuals in *Foxi3* cKO (n=17 follicles from 2 mice; 275 cells were scored) at 1st telogen; p=1.2 E-6. (E): Lef1 (red) and P-cadherin (green) staining at anagen onset showed decreased Lef1 activation *Foxi3* cKO compared to control mice (F): Representative images of Lhx2 staining in 1 year old mice. (G): Quantification of percent of hair follicles with malformations, as cysts and enlarged sebaceous glands, per optic field, at first telogen and at 1 year of age. The number of samples analyzed is the same as in (C). p (Control$^{1st\ telogen}$ vs. *Foxi3* cKO$^{1st\ telogen}$)=2.08 E-19; p (control$^{1y\ old}$ vs. *Foxi3* cKO$^{1y\ old}$)=9.0 E-25; p(*Foxi3* cKO$^{1st\ telogen}$ vs. *Foxi3* cKO$^{1y\ old}$)=0.013. Scale bar=50 μm. Data are shown as mean±SD. P-values were estimated using unpaired two-tailed Student t-test. The dotted line shows epithelial-mesenchymal border. Abbreviations: P=postnatal day; OF=optic field; ns=non-significant (p>0.05).

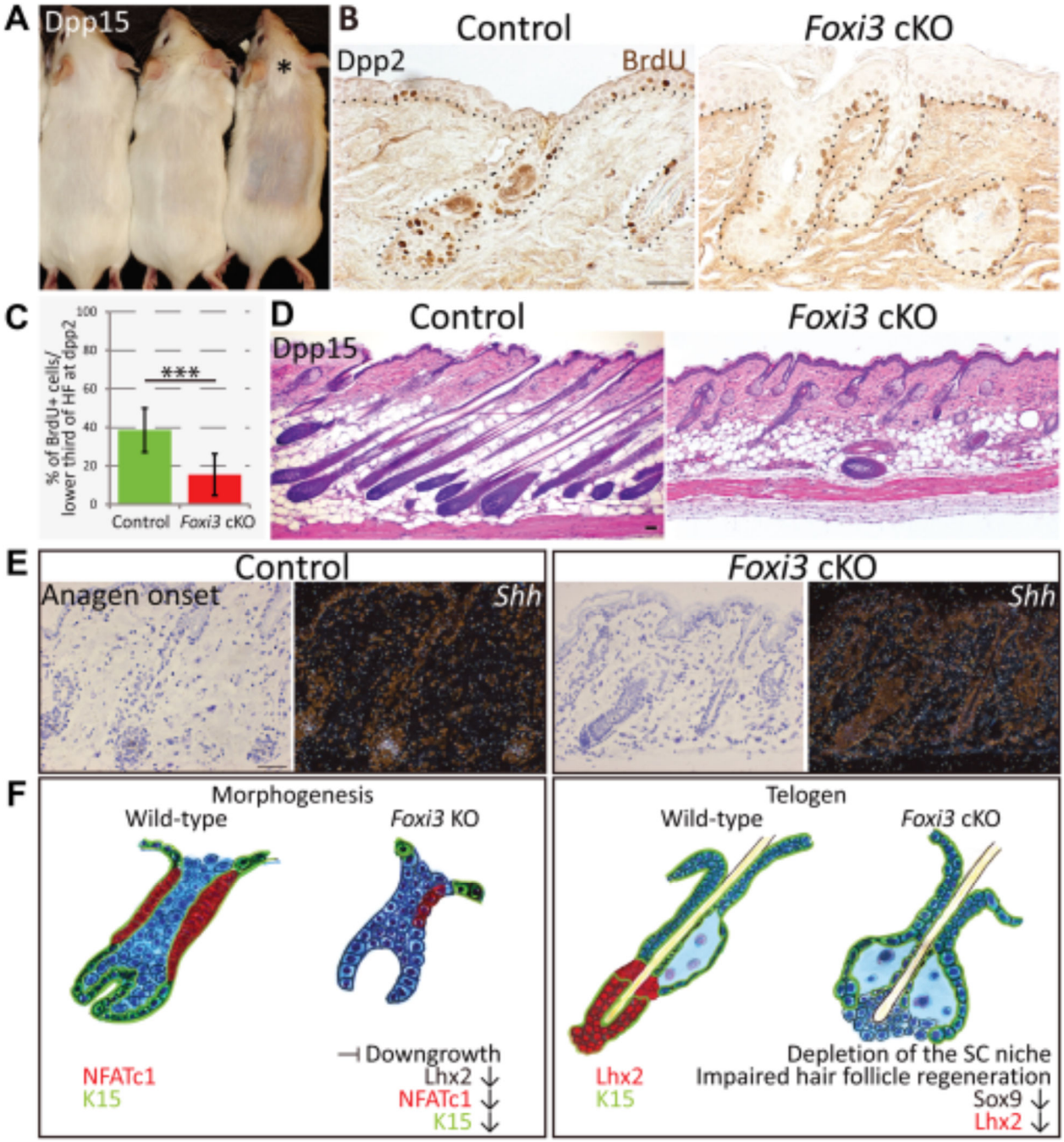

Figure 7.

Foxi3 deficiency compromises stem cell activation in a plucking-induced hair regeneration model. (A): Upon hair plucking, *Foxi3* cKO (marked with *) regrew hairs more slowly than controls. (B): Analysis of BrdU incorporation at day 2 post plucking (dpp2) revealed decreased cell proliferation in *Foxi3* cKO hair follicles. (C): Quantification of percent of BrdU+ cells in the lower third of the hair follicle at dpp2. Control (n=23 hair follicles, 1021 cells scored) and *Foxi3* cKO (n=28 hair follicles, 1149 cells scored); p=1.32 E-9. Data are shown as mean±SD. P-value was estimated using unpaired two-tailed Student t-test. (D): At

dpp15, *Foxi3* cKO mice showed only few follicles that had progressed to anagen while in littermate controls hair follicles had reached late anagen. (E): *Shh* expression in control and *Foxi3* cKO at the early stages of 1st anagen analyzed by radioactive in situ hybridization. In contrast to control littermates, *Shh* was not detectable in *Foxi3* cKO hair follicles. (F): A schematic summary describing the consequences of Foxi3 deficiency in embryonic hair follicle morphogenesis and in telogen hair follicles. The dermal component of the hair follicle was omitted for clarity.

Scale bar=50 μm. Abbreviations: Dpp=day post plucking; P=postnatal day.